Patent Docket:
70120-00005

IN THE UNITED STATES PATENT AND TRADEMARK OFFICE

In re the Application of:

Deniz K. Armani et al.

Serial No.: 10/678,354

Filed: October 2, 2003

For: ULTRA-HIGH Q MICRO-RESONATOR AND METHOD OF FABRICATION

Group Art Unit: 2828

Examiner: Tod Thomas Van Roy

INTERVIEW SUMMARY

Hon. Commissioner for Patents
P.O. Box 1450
Alexandria, VA 22313-1450

Sir:

The following is a summary of the Examiner Interview which took place telephonically on February 28, 2008.

INTERVIEW SUMMARY

The Interview took place telephonically on February 28, 2008, with the following individuals in telephonic attendance:

David M. Morse
Kerry J. Vahala
Deniz K. Armani
Examiner Tod Thomas Van Roy
Supervising Examiner Minsun Harvey

Prior to the interview, Applicants faxed the attached Interview Agenda, which included proposed claim amendments, the Declaration of Deniz K. Armani in support of Non-Obviousness, and exhibits thereto to the Examiner.

During the interview, the scope of the independent claims were discussed, including Applicants' proposed amendments, along with the teachings of the prior art and Applicants' assertion that the Armani Declaration negated a finding of obviousness. Applicants presented the arguments outlined in the Interview Agenda, but no agreement was reached regarding allowability of the claims. As such, although the attached documents were provided to the Examiner for review, they were not previously entered.

Respectfully submitted,

CONNOLLY BOVE LODGE & HUTZ LLP

DATE: May 9, 2008

By:
David M. Morse
Reg. No. 50,505

CONNOLLY BOVE LODGE & HUTZ LLP
1007 North Orange Street
P.O. Box 2207
Wilmington, Delaware 19899
(302) 658-9141
(302) 658-5614 (Fax)

Attachments:

Agenda For Applicant Initiated Interview, including proposed claim amendments and the Declaration of Deniz K. Armani, with attached Exhibits.

Patent Docket:
70120-00005

IN THE UNITED STATES PATENT AND TRADEMARK OFFICE

In re the Application of: Deniz K. Armani et al. Serial No.: 10/678,354 Filed: October 2, 2003 For: ULTRA-HIGH Q MICRO-RESONATOR AND METHOD OF FABRICATION	Group Art Unit: 2828 Examiner: Tod Thomas Van Roy

AGENDA FOR APPLICANT INITIATED INTERVIEW

Dear Examiner Van Roy:

I am writing to confirm the telephonic interview scheduled for Thursday, February 28, 2008, at 2 PM EST concerning the above-encaptioned patent application, and to provide an agenda for the meeting.

The following individuals, exclusive of USPTO personnel, are anticipated to participate in the telephone conferece:

David M. Morse, Applicants' Representative
Deniz K. Armani, Applicant
Kerry J. Vahala, Applicant

Submitted for your consideration as part of the interview process is the proposed claim amendments included below, and the Declaration of Deniz K. Armani, submitted in support of a finding of non-obviousness for the amended claims.

PROPOSED CLAIM AMENDMENTS

1. (Currently Amended) An ultra-high Q micro-cavity resonator, comprising:

an ultra-high Q micro-cavity having a Q value of at least 1.00 x 10^8, the micro-cavity being substantially planar; and

a substrate,

portions of the substrate located below the ultra-high Q micro-cavity being removed to form a pillar, the pillar supporting the ultra-high Q micro-cavity, whereby optical energy travels along an inner surface of the ultra-high Q micro-cavity.

2. (Cancelled)

3. (Original) The resonator of claim 1, the micro-cavity comprising an ultra-high Q silica micro-cavity.

4. (Original) The resonator of claim 1, the micro-cavity being substantially circular and having a diameter of about 10 micrometers to about 500 micrometers.

5. (Original) The resonator of claim 1, the micro-cavity having a toroid shape.

6. (Original) The resonator of claim 5, the toroid-shaped micro-cavity having a thickness of about five to about ten micrometers.

7. (Original) The resonator of claim 1, the micro-cavity having an elliptical shape.

8. (Original) The resonator of claim 1, the micro-cavity being substantially parallel to a top surface of the pillar.

9. (Canceled)

10. (Previously Presented) The resonator of claim 1, the micro-cavity having a Q value of about 10^8 to about 5×10^8.

11. (Previously Presented) The resonator of claim 1, the micro-cavity having a diameter of about 10 micrometers to about 30 micrometers and a Q value of about 500 million.

12. (Original) The resonator of claim 1, the micro-cavity comprising a glass material having a melting point that is lower than a melting point of the substrate.

13. (Original) The resonator of claim 1, a resonant mode within the micro-cavity comprising a whispering-gallery mode (WGM).

14. (Original) The resonator of claim 1, the substrate comprising a silicon substrate.

15. (Previously Presented) The resonator of claim 1, the substrate underneath the micro-cavity being removed by an etchant.

16. (Original) The resonator of claim 15, the etchant comprising a xenon difluoride (XeF_2) gas.

17. (Original) The resonator of claim 16, wherein the XeF_2 gas isotropically etches the substrate beneath a periphery of the micro-cavity to form the pillar.

18. (Original) The resonator of claim 17, the substrate comprising a silicon substrate.

19. (Original) The resonator of claim 1, the pillar having a tapered shape.

20. (Previously Presented) The resonator of claim 1, the micro-cavity including a rare earth dopant.

21. (Original) The resonator of claim 20, the rare Earth dopant being erbium, ytterbium, or neodymium.

22. (Previously Presented) The resonator of claim 1, the micro-cavity including an optically active component.

23. (Canceled)

24. (Canceled)

25. (Canceled)

26. (Canceled)

27. (Canceled)

28. (Original) The resonator of claim 1, the micro-cavity comprising a silica ultra-high Q micro-cavity, and the substrate comprising a silicon substrate.

29. (Currently Amended) An ultra-high Q micro-cavity resonator, comprising:

an optical material; and

a substrate that supports the optical material, wherein

the optical material is meltable by heat so that a periphery of the optical material adheres to itself to form an ultra-high Q micro-cavity having a Q value of at least 1.00 x 10^8, ~~and wherein~~

the micro-cavity is substantially planar, and

optical energy travels along an inner surface of the ultra-high Q micro-cavity.

30. (Original) The resonator of claim 29, the optical material comprising silica.

31. (Original) The resonator of claim 29, the optical material comprising a glass material having a melting point that is lower than a melting point of the substrate.

32. (Previously Presented) The resonator of claim 29, the optical material comprising a disk, wherein a diameter of the optical material becomes smaller when heated to form a disk.

33. (Previously Presented) The resonator of claim 32, wherein the diameter decreases until the molten optical material collapses after which the diameter remains substantially constant.

34. (Cancelled)

35. (Original) The resonator of claim 29, the ultra-high Q micro-cavity comprising an ultra-high Q silica micro-cavity.

36. (Original) The resonator of claim 29, the ultra-high Q micro-cavity being substantially circular and having a diameter of about 10 micrometers to about 500 micrometers

37. (Original) The resonator of claim 29, the ultra-high Q micro-cavity having a toroid shape.

38. (Original) The resonator of claim 37, the toroid having a thickness of about five to about ten micrometers.

39. (Original) The resonator of claim 29, the ultra-high Q micro-resonator having an elliptical shape.

40. (Original) The resonator of claim 29, the ultra-high Q micro-cavity being substantially parallel to a top surface of the pillar.

41. (Original) The resonator of claim 29, wherein a size of the ultra-high Q micro-cavity is limited by a size of a top surface of the substrate.

42. (Canceled)

43. (Previously Presented) The resonator of claim 29, the ultra-high Q micro-cavity having a Q value of about 10^8 to about 5×10^8.

44. (Previously Presented) The resonator of claim 29, the ultra-high Q micro-cavity having a diameter of about 10 micrometers to about 30 micrometers and a Q value of about 500 million.

45. (Original) The resonator of claim 29, a resonant mode within the ultra-high Q micro-cavity being a whispering-gallery mode (WGM).

46. (Original) The resonator of claim 29, the substrate comprising a silicon substrate.

47. (Original) The resonator of claim 29, wherein portions of the substrate located below the ultra-high Q micro-cavity are removed to form a pillar, the pillar supporting the ultra-high Q micro-cavity.

48. (Previously Presented) The resonator of claim 47, the pillar having a tapered shape.

49. (Previously Presented) The resonator of claim 29, the substrate underneath the periphery of the ultra-high Q micro-cavity being removed by an etchant.

50. (Original) The resonator of claim 49, the etchant comprising xenon difluoride (XeF_2) gas.

51. (Original) The resonator of claim 50, wherein the XeF_2 gas isotropically etches the substrate beneath the periphery of the micro-cavity.

52. (Original) The resonator of claim 29, the heat source comprising an Excimer laser.

53. (Previously Presented) The resonator of claim 52, wherein the Excimer laser heats and liquefies the optical material.

54. (Original) The resonator of claim 29, the heat source comprising a CO_2 laser.

55. (Original) The resonator of claim 54, wherein the CO_2 laser emits radiation having a wavelength of about 10.6 micrometers.

56. (Original) The resonator of claim 54, wherein the CO_2 laser heats the optical material for about 1 microsecond to about 10 seconds.

57. (Original) The resonator of claim 54, wherein the CO_2 laser heats and liquefies the optical material.

58. (Original) The resonator of claim 29, wherein the optical material comprises silica and the substrate comprises silicon.

59. (Canceled)

60. (Previously Presented) The resonator of claim 29, the ultra-high Q micro-cavity including a dopant.

61. (Original) The resonator of claim 60, the dopant being erbium, ytterbium, or neodymium.

62. (Previously Presented) The resonator of claim 29, the ultra-high Q micro-cavity including an optically active component.

63. (Canceled)

64. (Canceled)

65. (Canceled)

66. (Canceled)

67. (Previously Presented) A planar micro-cavity resonator, comprising:

an ultra-high Q toroid-shaped planar silica micro-cavity having a Q value of at least 1.00 x 10^8; and

a silicon substrate;

wherein portions of the silicon substrate located below a periphery of the ultra high-Q toroid-shaped planar silica micro-cavity are isotropically etched to form a silicon pillar, the silicon pillar supporting the ultra-high Q toroid-shaped planar silica micro-cavity, and wherein light energy traverses along an inner surface of the ultra-high Q toroid-shaped planar micro-cavity.

68. (Withdrawn) A method of forming an ultra-high Q micro-cavity, comprising:

providing a substrate and an optical material;

etching the substrate to form a pillar, the pillar supporting the optical material; and

heating a periphery of the optical material so that the periphery melts and adheres to itself to form the ultra-high Q micro-cavity having a Q value of at least 1.00 x 10^8, whereby optical energy travels along an inner surface of the ultra-high Q micro-cavity.

69. (Withdrawn) The method of claim 68, providing the substrate further comprising providing a silicon substrate.

70. (Withdrawn) The method of claim 69, wherein etching the silicon substrate to form a silicon pillar further comprises isotropically etching the silicon substrate with a xenon difluoride gas.

71. (Withdrawn) The method of claim 69, providing the optical material further comprising providing silica (SiO2).

72. (Withdrawn) The method of claim 69, wherein heating the periphery of the optical material further comprises heating the periphery with an Excimer laser.

73. (Withdrawn) The method of claim 72, wherein heating the periphery with the Excimer laser further comprises liquefying the optical material.

74. (Withdrawn) The method of claim 69, wherein heating the periphery of the optical material further comprises heating the periphery with a CO_2 laser.

75. (Withdrawn) The method of claim 74, wherein heating the periphery with the CO_2 laser further comprises heating the periphery with the CO_2 laser at a wavelength of about 10.6 micrometers.

76. (Withdrawn) The method of claim 74, wherein heating the periphery with the CO_2 laser further comprises heating the periphery for about 1 microsecond to about 10 seconds.

77. (Withdrawn) The method of claim 74, wherein heating the periphery with the CO_2 laser further comprises liquefying the optical material.

78. (Currently Amended) A micro-cavity resonator, comprising:

an ultra-high Q micro-cavity having a Q value of at least 1.00 x 10^8 and having a biotinylated surface, the micro-cavity being substantially planar; and

a substrate, portions of the substrate located below the ultra-high micro-cavity being removed to form a pillar that supports the ultra-high Q micro-cavity, whereby optical energy travels along an inner surface of the micro-cavity.

79. (Previously Presented) An ultra-high Q micro-cavity resonator, comprising:

an optical material; and

a substrate that supports the optical material, wherein

the optical material is meltable by a heat source so that a periphery of the optical material adheres to itself to form an ultra-high Q micro-cavity, the ultra-high Q micro-cavity having a Q value of at least 1.00 x 10^8 and having a biotinylated surface, ~~and wherein~~

the micro-cavity is substantially planar, and

optical energy travels along an inner surface of the ultra-high Q micro-cavity.

80. (Withdrawn) The method of claim 68, further comprising etching the optical material.

81. (Previously Presented) The ultra-high Q micro-cavity resonator of claim 1 having a root mean square (rms) roughness of several nanometers.

82. (Previously Presented) The ultra-high Q micro-cavity resonator of claim 29 having a root mean square (rms) roughness of several nanometers.

INTERVIEW AGENDA

At the scheduled interview, Applicants intent to discuss the following:

1. The proposed claim amendments in view of the prior art of record. Each of the independent claims, namely claims 1, 29, 67, 78, and 79, in the application now include limitations indicating that the micro-cavity is substantially planar or planar.

2. The Declaration of Deniz K. Armani in Support of Non-Obviousness. This Declaration and the accompanying exhibits have been submitted as evidence to support Applicants' assertion that the proposed amended claims are not obvious on the basis that the prior art of record could not be modified with a reasonable expectation of success to create the subject matter of the claims. A reasonable expectation of success is a requirement of establishing a prima facie case of obviousness. *See* MPEP § 2143.02; *See also*, *In re Dow Chemical Co.*, 837 F.2d 469, 473, 5 U.S.P.Q.2d (BNA) 1529, 1531 (Fed. Cir. 1988) ("Both the suggestion and the expectation of success must be founded in the prior art, not in applicant's disclosure."); *In re O'Farrell*, 853 F.2d 894, 903, 7 USPQ2d 1673, 1681 (Fed. Cir. 1988) (evidence suggesting the modification to prior art would be successful was a key factor in a finding of obviousness.).

Here, Applicants present evidence showing that, at the time the present application was filed and for at least 5 years afterward, other independent studies confirm that attempts have been made to fabricate planar microresonators, and that those attempts have resulted in planar microresonators having Q factors of no more than 3 magnitudes less than what is described and claimed in the present application.

In view of this evidence, Applicants submit that when the respective teachings of the prior art of record are considered, a person of skill in the art would have no reasonable expectation of successfully fabricating a substantially planar or planar microresonator having a Q factor of at least 1.00×10^8 on a substrate.

Applicants and the undersigned thank the Examiner for taking the time to review these materials in advance of the Interview.

Respectfully submitted,

CONNOLLY BOVE LODGE & HUTZ LLP

DATE: February 25, 2008

By: ____________________
David M. Morse
Reg. No. 50,505

CONNOLLY BOVE LODGE & HUTZ LLP
The Nemours Building
1007 North Orange Street
P.O. Box 2207
Wilmington, Delaware 19899
(302) 658-9141
(302) 658-5614 (Fax)

Patent Docket:
70120-00005

IN THE UNITED STATES PATENT AND TRADEMARK OFFICE

In re the Application of:	Group Art Unit: 2828
Deniz K. Armani et al.	Examiner: Tod Thomas Van Roy
Serial No.: 10/678,354	
Filed: October 2, 2003	
For: ULTRA-HIGH Q MICRO-RESONATOR AND METHOD OF FABRICATION	

DECLARATION OF DENIZ K. ARMANI SUBMITTED IN SUPPORT OF NON-OBVIOUSNESS

I, Deniz K Armani, one of the named inventors in the above-encaptioned patent application, hereby declare as follows:

1. I am familiar with the timeline associated with the development of the technology disclosed in the present application and the subsequent publication reporting on the technological developments. The present application claims priority to U.S. Provisional Application Serial No. 60/415,412, filed October 2, 2002 (hereinafter the "Priority Application"). The technological developments disclosed in the present application were publicly reported in an article published as D. K. Armani et al., "Ultra high-Q toroid microcavity on a chip," *Nature*, Vol. 421, pp. 925–929, Feb. 2003 (hereinafter the "*Nature* Article").

2. I have reviewed the article entitled "Ultrahigh-quality-factor silicon-on-insulator microring resonator", as published by Jan Niehusmann et al. in *Optics Letters*, Vol. 29, No. 24, December 15, 2004, a true and correct copy of which is attached as Exhibit 1.

Niehusmann et al. describe the development of Silicon-on-insulator (SOI) microring resonators.

3. Niehusmann et al. state that SOI integrated technology is anticipated to be highly beneficial for the convergence of microelectronics and photonics because due to cost savings that can be realized by integrating photonic and electronic functions on the same substrate. These same benefits were understood, but not fully realized, in October 2002 when the Priority Application was filed. This article also describes possible applications for microring resonators having a "high Q factor" or a "very high Q factor", such as for telecommunication applications in providing wavelength selective filtering, add-drop multiplexing, compact dispersion compensation, and frequency-selective coupling, or for chemical or biomolecule sensor applications, or even to enhance evanescent-field fluorescence sensing.

4. The Q factor reported for the SOI microring resonators developed by Niehusmann et al. were 139.000 ± 6.000. These SOI microring resonators were fabricated directly on a substrate, and Niehusmann et al. reported that the Q factor was "much higher than [any Q factor values that] have been reported up to now" for integrated microring resonators. Niehusmann et al. recognized a single exception to their statement based upon SOI microring resonators fabricated by utilizing surface tension in the materials generated by a melting process. In recognizing this exception, Niehusmann et al. cited to the *Nature* Article. Moreover, Niehusmann et al. stated in the abstract of the paper that:

> "These [(the Q factor reported)] are *believed to be the highest values reported* for a curved SOI waveguide device and for any directly structured semiconductor microring fabricated without additional melting-induced surface smoothing."

(Emphasis added.)

5. I have reviewed the article entitled "Silicon Microtoroidal Resonators With Integrated MEMS Tunable Coupler", as published by Jin Yao et al. in *IEEE Journal Of Selected Topics In Quantum Electronics*, Vol. 13, No. 2, March/April 2007, a true and correct copy of which is attached as Exhibit 2. Yao et al. describe an silicon microtoroidal resonator integrated on a substrate with a tunable optical coupler.

6. In this 2007 paper, Yao et al. report a process for fabricating a microtoroidal resonator integral to a substrate that also includes a MEMS-actuated tunable optical coupler. The process used to fabricate the microtoroidal resonator is a hydrogen annealing process, which enables creation of the microtoroidal structure and preserves the desired optical qualities of the microtoroidal resonator. The unloaded Q factor achieved by this fabrication process is reported to be as high as 1.0×10^5. Yao et al. indicate that very high Q factors have been demonstrated in SiO^2, but that because of the thermal reflow process used to create such microtoroidal resonators, such processes cannot be applied to integrated SOI photonics devices. The thermal reflow process referred to by Yao et al. is the one described in the *Nature* Article authored by the named inventors of the present application, which produces microtoroidal resonators having Q factors as high as 5×10^8.

7. Through my work in developing the technology disclosed in the present application, I am now and was, at the time the Priority Application was filed, familiar with the state of the art for microring and microdisk resonators. When the Priority Application was filed, I was aware of microdisk resonators having Q factors as high as 17,000. Those microdisk resonators were constructed from GaAs formed into disks upon a pedestal formed from a substrate AlGaAs. The article reporting and describing these microdisk resonators was included as part of the Information Disclosure Statement filed on March 1, 2004 as cite No. 7 in the Non-Patent Literature Documents section of form PTO/SB/08B. I was also aware of microring resonators having Q factors as high as 13,000. Those microring resonators were constructed from polymers forming a

microring on a silicon substrate (but not on a pedestal). The article reporting and describing these microdisk resonators was included as part of the Information Disclosure Statement filed on March 1, 2004 as cite No. 12 in the Non-Patent Literature Documents section of form PTO/SB/08B. At the time the Priority Application was filed, I was not aware, nor am I currently aware, of any other microring or microdisk resonators achieving Q factors approaching within three orders of magnitude of 10^7, other than those fabricated using the techniques developed by myself and my co-inventors.

8. I have reviewed U.S. Patent No. 6,259,717 to Stone et al., which is part of the prosecution record for the present patent application. Stone et al. do not disclose any of microring resonators, microtoroidal resonators, or any other type of substantially planar microresonator. Rather, Stone et al. disclose deformed cylindrical resonators and prolate spheroidal resonators as shown in Figs. 3a & 3b, respectively. Moreover, Fig. 5, which is a plot obtained by numerical solutions to the wave equation, illustrates *anticipated* Q factors for a cylindrical asymmetric resonant cavity only. As such, the stated theoretical values for such a cylindrical resonator are inapplicable to Q factors achievable for microring resonators.

9. I further declare under penalty of perjury that all statements made herein of my own knowledge are true and that all statements made on information and belief are believed to be true; and further that these statements are made with the knowledge that willful false statements and the like so made are punishable by fine or imprisonment, or both, under Title 18, United States Code § 1001, and that such willful false statements may jeopardize the validity of the application or any patent issuing thereon.

DATE: 2/12/2008 By: ______________________
Deniz K. Armani

EXHIBIT 1

Ultrahigh-quality-factor silicon-on-insulator microring resonator

Jan Niehusmann, Andreas Vörckel, and Peter Haring Bolivar

Institut für Halbleitertechnik, Rheinisch-Westfälische Technische Hochschule Aachen, Sommerfeldstrasse 24, 52056 Aachen, Germany

Thorsten Wahlbrink and Wolfgang Henschel

Advanced Micro-electronic Center Aachen (AMICA), AMO GmbH, Huyskensweg 25, 52074 Aachen, Germany

Heinrich Kurz

Institut für Halbleitertechnik, Rheinisch-Westfälische Technische
Hochschule Aachen, Sommerfeldstrasse 24, 52056 Aachen, Germany, and
Advanced Micro-electronic Center Aachen (AMICA), AMO GmbH, Huyskensweg 25, 52074 Aachen, Germany

Received May 27, 2004

The development of ultrahigh-quality-factor (Q) silicon-on-insulator (SOI) microring resonators based on silicon wire waveguides is presented. An analytical description is derived, illustrating that in addition to low propagation losses the critical coupling condition is essential for optimizing device characteristics. Propagation losses as low as 1.9 ± 0.1 dB/cm in a curved waveguide with a bending radius of 20 μm and a Q factor as high as 139.000 ± 6.000 are demonstrated. These are believed to be the highest values reported for a curved SOI waveguide device and for any directly structured semiconductor microring fabricated without additional melting-induced surface smoothing. © 2004 Optical Society of America

OCIS codes: 130.3120, 230.5750.

Silicon-on-insulator (SOI) technology is a promising platform for the convergence of microelectronics and photonics. It has a large potential given the high photonic integration capabilities that are made possible by the high refractive-index contrast between silicon and typical cladding materials, the natural vertical confinement of optical waves given by the buried oxide layer, and the potential cost-efficient integration of photonic and electronic functions on the same substrate given by silicon technology.[1,2] However, at the same time, these beneficial characteristics lead to stringent manufacturing tolerances and a high sensitivity to surface roughness, as the higher refractive index of silicon in comparison with silica implies smaller silicon wire waveguide dimensions.[3] It is therefore critical to optimize manufacturing tolerance and to minimize surface roughness to facilitate useful low-loss SOI photonic solutions.[4]

In this Letter we present the development of high-quality SOI microring resonators based on silicon wire waveguides. These microrings can find direct application in the areas of telecommunication, sensors, quantum electrodynamics, and nonlinear optics.[5] For telecommunication, microrings have a multitude of applications, allowing wavelength-selective filtering, add–drop multiplexing, compact dispersion compensation, and frequency-selective coupling in optical networks.[6–8] Additionally, microrings are excellent model systems for deriving fundamental properties of curved waveguides as a crucial building block of photonic integrated circuits. Here we demonstrate a microring resonator with maximized quality factor Q to illustrate and quantify the low loss that can be achieved by use of an improved SOI process technology. Although the high Q factor demonstrated here surpasses typical needs of actual telecommunication data channels, the associated low loss is an indicator of the large degree of freedom in the future design of more complex and very large scale integrated telecommunication components that can be achieved with advanced SOI waveguide technology.

Microrings with a very high Q factor can also be used directly for sensor applications, where the dielectric loading and concomitant frequency shift of a resonator are used to monitor chemicals or biomolecules[9,10] or the higher field in the resonator is used to enhance evanescent-field fluorescence sensing.[11] In this type of application higher Q factors allow smaller resonance shifts to be detected. The internal field enhancement also increases sensitivity. Ultrahigh-Q optical microcavities with Q factors of up to 8×10^9 were recently demonstrated by use of microspheres.[12] However, these and similarly attractive microtoroids demonstrated in silicon[13] make use of the formation of ultraflat surfaces on the spheres and (or) microtoroids by using the surface tension during a melting process. This makes integration into photonic circuits and the dimensional control of the device during manufacture problematic. Here we present directly structured SOI-based microring resonators with Q factors that are much higher than have been reported up to now.

For proper design and optimization of a high-quality resonator, several aspects have to be considered. Most obviously, a sharp resonance, i.e., a high Q, is desired to observe small resonance wavelength shifts, which is necessary for sensing or switching applications. The

0146-9592/04/242861-03$15.00/0 © 2004 Optical Society of America

Q factor of a microring resonator coupled to a single waveguide is given by

$$Q = \frac{2\pi n_{\mathrm{eff}}}{\lambda_0} \frac{L}{2 \arccos\{[1 - 4t/\tau + (t/\tau)^2]/(-2t/\tau)\}} = \frac{\lambda_0}{\Delta\lambda_{3\,\mathrm{dB}}}, \tag{1}$$

where n_{eff} is the effective index of refraction of the propagating mode in the microring, λ_0 is the resonance wavelength, L is the length of the microring, t is the field transmission coefficient at the waveguide–resonator coupling, and $\tau = \exp(-\alpha L/2)$ is the attenuation of the field per round trip for a microring resonator with attenuation constant α.[14] A reasonably noticeable shift of the resonance wavelength should be of the order of $\Delta\lambda_{\mathrm{detect}} \approx 1/2\,\Delta\lambda_{3\,\mathrm{dB}}$. Thus it is evident that high Q factors are necessary for sensitive switching or sensing devices. The Q factor of an actual device depends on the chosen geometry, which determines parameters t, L, and n_{eff} in Eq. (1), and on the propagation losses in the ring, which determine τ.

For $t\tau$ close to 1, Eq. (1) can be approximated by

$$Q = \frac{2\pi n_{\mathrm{eff}}}{\lambda_0} \frac{L}{-2 \ln t\tau}; \tag{2}$$

i.e., Eq. (1) is dependent on the product $t\tau$, which sums up propagation and coupling losses. Coupling losses are a free design parameter. Hence it is useful to estimate the maximum achievable Q factor that can be achieved with a given technology from the propagation loss $\alpha = -2(\ln \tau/L)$ inside the cavity. Neglecting the coupling loss to external waveguides, the maximum achievable Q factor can easily be determined from Eq. (2) as

$$Q_{\mathrm{limit}} = \frac{2\pi n_{\mathrm{eff}}}{\lambda_0} \frac{L}{-2 \ln \tau} = \frac{2\pi n_{\mathrm{eff}}}{\lambda_0} \frac{1}{\alpha}. \tag{3}$$

Minimizing losses is therefore of prime importance for the development of ultrahigh-Q microcavities. In the case of SOI-based waveguide technology, low propagation losses can only be achieved with ultrasmooth waveguide surfaces, requiring specific optimized processing steps.

For reliable detection of a resonance shift or switching event, a large throughput attenuation of the signal of the coupled waveguide as a result of the resonance in the microring is necessary. This can be achieved by critical coupling, where complete throughput attenuation at resonance is achieved. The condition for critical coupling is given by $t = \tau$ in Eq. (1).[14] In that case the Q factor of the microcavity is given by $Q_{\mathrm{critical}} = Q_{\mathrm{limit}}/2$. Thus, for practical sensor applications only half the maximum Q factor that is possible as a result of the propagation loss can be used effectively.

A further technical parameter of importance is the cavity field enhancement. For applications based on a nonlinear material response, such as photonic switching, stronger fields inside the resonator induce larger shifts of the resonance wavelength, lowering, e.g., switching thresholds. The field enhancement factor at critical coupling conditions is given by

$$\mathrm{FE}_{\mathrm{critical}} = \frac{1}{\sqrt{1 - \tau^2}}. \tag{4}$$

Here again, the maximum field enhancement coincides with a low propagation loss per round trip in the cavity. Therefore low propagation losses are the key issue in addressing most of the general requirements of microring resonators.

Several wire waveguide microrings based on SOI technology have been reported.[6,14] However, because of technological restrictions, the Q factor has been limited to values of the order of 2.500. Two aspects are optimized here, in comparison to former approaches[14]: an optimization of the pattern generation during electron-beam lithography (EBL) is performed, and the surface roughness during pattern transfer to the silicon waveguides is optimized. The waveguides are fabricated on SOI substrates consisting of a 1-μm-thick buried oxide layer and a 0.45-μm-thick device layer. For the waveguides a width of 0.5 μm has been chosen. The devices are defined by EBL using hydrogen silsesquioxane as an EBL resist.[15] Corrections are performed on the EBL pattern generation by preprocessing the microring into minimal feature size polygons. This minimizes the rectangular discontinuities that are characteristic of standard pattern generation of curved structures and that can reach several tens of nanometers. Pattern transfer is achieved by HBr inductive coupled reactive-ion etching, which selectively stops at the Si/SiO$_2$ interface, optimizing the etching parameters to minimize surface roughness. The input and output facets of the waveguides are prepared by cleaving the sample. A scanning electron microscope image of a typical device is depicted in Fig. 1.

For device characterization a commerical measurement setup consisting of a tunable external cavity diode laser and a photodiode is used. TM-polarized light (electric field perpendicular to the device plane) is butt coupled to the input by a polarization-maintaining optical fiber. The light at the throughput waveguide is

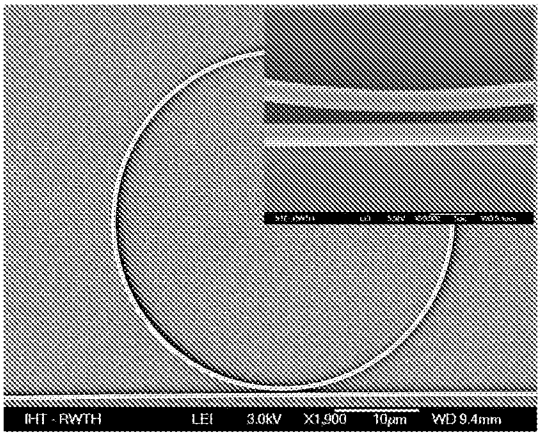

Fig. 1. Scanning electron micrographs of a SOI microring resonator with a radius of 20 μm, including an overview and a coupling region closeup (inset).

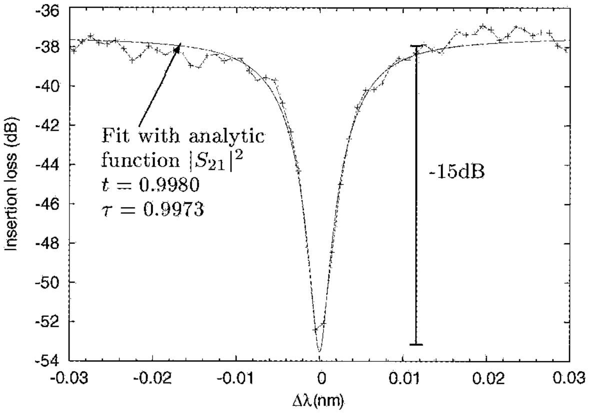

Fig. 2. Measured insertion loss and fit of analytical transfer function of a SOI microring resonator of radius $r = 20\ \mu$m, with $\Delta\lambda = \lambda - 1547.680$ nm.

butt coupled to a multimode fiber connected to a photodetector. The analytical transfer function of the device is given by[14]

$$|S_{21}|^2 = \frac{t^2 - 2t\tau \cos \phi + \tau^2}{1 - 2t\tau \cos \phi + (t\tau)^2}, \tag{5}$$

where $\phi = 2\pi(L_{\mathrm{eff}}/\lambda) = (4\pi^2 r_{\mathrm{eff}} n_{\mathrm{eff}})/\lambda$ is the phase shift per round trip around the resonator. Figure 2 shows the measured insertion loss spectrum of a SOI microring resonator with a radius of $r = 20\ \mu$m and a gap of 0.25 μm between the microring resonator and the adjacent waveguide. The analytical transfer function $|S_{21}|^2$ is fitted to the resonance at the wavelength $\lambda = 1547.68$ nm, and $n_{\mathrm{eff}} = 2.5864$ is derived from the resonance wavelengths. The fit yields values of $t = 0.9980 \pm 0.0002$ and $\tau = 0.9973 \pm 0.0001$, demonstrating that favorable critical coupling has nearly been achieved. Therefore a significant throughput attenuation of -15 dB at resonance is observed. The superposed oscillation is due to Fabry–Perot effects in the periphery of the device. As $|S_{21}|^2$ is invariant to commutation of t and τ, we chose the conservative values where $t > \tau$; i.e., attenuation of the wave propagating through the ring is higher than coupling from the ring to the waveguide. This choice does not influence the Q factor, but it means that the propagation loss may actually be even lower than calculated below.

Applying Eq. (1) to the fitted parameters yields a Q factor of $Q \approx 139.000 \pm 6.000$, which agrees with a direct linewidth estimation. As an illustration, this means that using this resonator as a sensor allows the detection of a resonance wavelength shift as low as $\Delta\lambda_{\mathrm{detect}} \approx 0.006$ nm, which can easily be detected as a -3-dB signal change. This wavelength shift corresponds to a shift of the effective refractive index of as low as $\Delta n_{\mathrm{eff,detect}} \approx 1.7 \times 10^{-5}$.

Taking τ obtained from the fit of $|S_{21}|^2$ to the experimental data and the length L of the device, the propagation loss inside the microring resonator can be deduced from

$$\alpha\left[\frac{\mathrm{dB}}{\mathrm{cm}}\right] = \frac{-2 \times 10^5 \log_{10}(\tau)}{L[\mu\mathrm{m}]}. \tag{6}$$

For the resonance shown in Fig. 2, Eq. (6) gives a propagation loss of $\alpha \approx 1.9 \pm 0.1$ dB/cm. To our knowledge this is the lowest propagation loss reported for a SOI ring resonator or any curved SOI wire waveguide fabricated by reactive-ion etching without any further smoothing steps [e.g., melting and (or) thermal oxidation]. This result is similar to the best values reported for straight SOI waveguides.[16]

In summary, we have presented the design, fabrication, and optical characterization of ultrahigh-Q SOI microring resonators. We illustrate that, in addition to a minimization of losses to attain a high Q factor, the condition of critical coupling is of fundamental relevance for achieving high-efficiency devices. We demonstrate the development of microring resonators based on an optimized SOI fabrication technology, yielding what is to our knowledge the highest Q factor of 139.000 ± 6.000 and the lowest propagation loss without additional smoothing steps ever reported for SOI ring resonator technology.

The authors thank P. Kersten for motivating this work. This work was supported by European Commission contract IST-2001-38919 (PHOENIX) and the Ministerium für Wissenschaft und Forschung des Landes Nordrhein Westfalen. J. Niehusmann's e-mail address is niehusmann@iht.rwth-aachen.de.

References

1. B. N. Kurdi and D. G. Hall, Opt. Lett. **13,** 175 (1988).
2. R. A. Soref, Proc. IEEE **81,** 1687 (1993).
3. K. K. Lee, D. R. Lim, H.-C. Luan, A. Agarwal, J. Foresi, and L. C. Kimerling, Appl. Phys. Lett. **77,** 1617 (2000).
4. T. Tsuchizawa, T. Watanabe, E. Tamechika, T. Shoji, K. Yamada, J. Takahashi, S. Uchiyama, S. Itabashi, and H. Morita, in *LEOS Annual Meeting* (Lasers and Electro-Optics Society, Piscataway, N.J., 2002), p. 287.
5. K. J. Vahala, Nature **424,** 839 (2003).
6. B. E. Little, J. S. Foresi, G. Steinmeyer, E. R. Thoen, S. T. Chu, H. A. Haus, E. P. Ippen, L. C. Kimerling, and W. Greene, IEEE Photon. Technol. Lett. **10,** 549 (1998).
7. B. E. Little, S. T. Chu, W. Pan, and Y. Kokubun, IEEE Photon. Technol. Lett. **12,** 323 (2000).
8. L. Eldada, Rev. Sci. Instrum. **75,** 575 (2004).
9. C.-Y. Chao and L. J. Guo, Appl. Phys. Lett. **83,** 1527 (2003).
10. E. Krioukov, D. J. W. Klunder, A. Driessen, J. Greve, and C. Otto, Opt. Lett. **27,** 512 (2002).
11. S. Blair and Y. Chen, Appl. Opt. **40,** 570 (2001).
12. D. W. Vernooy, V. S. Ilchenko, H. Mabuchi, E. W. Streed, and H. J. Kimble, Opt. Lett. **23,** 247 (1998).
13. D. K. Armani, T. J. Kippenberg, S. M. Spillane, and K. J. Vahala, Nature **421,** 925 (2003).
14. A. Vörckel, M. Mönster, W. Henschel, P. Haring Bolivar, and H. Kurz, IEEE Photon. Technol. Lett. **15,** 912 (2003).
15. W. Henschel, Y. M. Georgiev, and H. Kurz, J. Vac. Sci. Technol. B **21,** 2018 (2003).
16. P. Dumon, W. Bogaerts, J. Van Campenhout, V. Wiaux, J. Wouters, S. Beckx, and R. Baets, in *LEOS Annual Meeting* (Lasers and Electro-Optics Society, Piscataway, N.J., 2003), p. 289.

EXHIBIT 2

Silicon Microtoroidal Resonators With Integrated MEMS Tunable Coupler

Jin Yao, David Leuenberger, Ming-Chang M. Lee, *Member, IEEE*, and Ming C. Wu, *Fellow, IEEE*

***Abstract*—A single crystalline silicon microtoroidal resonator with integrated MEMS-actuated tunable optical coupler is demonstrated for the first time. It is fabricated by combining hydrogen annealing and wafer bonding processes. The device operates in all three coupling regimes: under-, critical, and over-coupling. We have also developed a comprehensive model based on time-domain coupling theory. The experimental and theoretical results agree very well. The quality factor (Q) is extracted by fitting the experimental curve with the model. The unloaded Q is as high as 110 000, and the loaded Q is continuously tunable from 110 000 to 5400. The extinction ratio of the transmittance is 22.4 dB. This device can be used as a building block of resonator-based reconfigurable photonic integrated circuits.**

***Index Terms*—Integrated optics, optical resonators, surface roughness, tunable.**

I. INTRODUCTION

OPTICAL microresonators are key enabling elements for compact filters [1], lasers [2], electro-optic modulators [3], add–drop multiplexers [4], optical dispersion compensators [5], delay lines [6], nonlinear optical devices [7], and optical sensors [8], [9]. The performance of microresonators depends on two parameters: the quality factor (Q) of the resonator and the coupling ratio between the waveguides and the resonator (κ). Microfabricated resonators with very high Q has been demonstrated in SiO_2 [10] and Si [11]. The coupling ratio needs to be controlled precisely to achieve optimum performance [12]. This has been achieved by adjusting prism couplers in fused silica microsphere resonators [13] or by moving tapered fiber couplers [14]–[16] with piezo-controlled micropositioners. However, such setups are bulky and cannot be integrated. In microresonators with integrated waveguides, the coupling ratio is determined by the fabrication process [17]. The value of κ or, perhaps more importantly, its relation with the cavity Q, cannot be controlled precisely. Some trimming processes have been proposed to control the resonance frequency, but not κ [18], [19].

Recently, microresonators with tunable coupling ratios have been reported [20]–[23]. A Mach–Zehnder interferometer (MZI) has been integrated with a racetrack resonator [20]. The resonator can operate in all coupling regimes (uncoupled, under-, critical, or over-coupled). An unloaded Q of 1.9×10^4 and an On–Off ratio of 18.5 dB have been achieved. However, the circumference of the resonator is rather large (1430 μm) due to the long MZI structure, which limits the free spectral range and the footprint that it can achieve. Recently, microfluidic approach has also been employed to tune both the resonance wavelength and the coupling ratio of low-index microring resonators made in SU8 [23]. The refractive index of the surrounding media was varied by mixing two different liquids. Critical coupling with an extinction ratio of 37 dB have been attained. However, index variation is small (~ 0.04), which limits the tuning range of κ. In addition, the tuning speed is slow (~ 2 s) and the fluidic packaging is cumbersome.

Previously, we have reported the first silicon microdisk resonator with integrated microelectromechanical systems (MEMS) tunable coupler [21], [22]. By physically changing the gap spacing between the waveguide and the resonator, κ can be varied over a wide range (0 to 34%) and a high Q (100 000) have been achieved simultaneously. Tunable dispersion compensators (185 to 1200 ps/nm) have also been demonstrated [22]. One drawback of that device is the lack of radial mode control in microdisk resonators, which could produce additional resonances due to high-order modes. In this paper, we report on the first single crystalline silicon *microtoroidal* resonator with MEMS tunable optical coupler. Microtoroidal resonators offer tighter confinement of the optical mode and eliminate multiple radial modes observed in microdisks. Microtoroidal resonators have been made in SiO_2 by thermal reflow [10], however, such process cannot be applied to single crystalline structures. Instead, we use hydrogen annealing to create three-dimensional toroidal structures while preserving the single crystalline quality [24]. To integrate the microtoroidal resonators with MEMS tunable waveguides, we have combined the hydrogen annealing process with wafer bonding technique. All the three coupling regimes have been demonstrated, with the loaded Q tunable from 110 000 to 5400.

II. DEVICE DESIGN AND FABRICATION

A. Device Structure Design

The schematic of the tunable microtoroidal resonator is shown in Fig. 1. Two suspended waveguides are vertically coupled to a microtoroidal resonator. It is realized on a two-layer silicon-on-insulator (SOI) structure. The microtoroid and the fixed electrodes of the MEMS actuators are fabricated on the lower SOI layer, while the suspended waveguides are integrated on the upper SOI. The initial spacing between the microtoroid and the

---

Manuscript received October 2, 2006; revised February 12, 2007. This work was supported in part by the Defense Advanced Research Project Agency (DARPA) University Photonics Research (UPR) Program HR0011-04-1-0040. The work of D. Leuenberger was supported by a one-year fellowship from the Swiss National Science Foundation, in 2005.

J. Yao and M. C. Wu are with the Department of Electrical Engineering and Computer Sciences, University of California, Berkeley, CA 94720 USA (e-mail: jinyao@eecs.berkeley.edu; wu@eecs.berkeley.edu).

D. Leuenberger is with the Integrated Photonics Laboratory, University of California, Berkeley, CA 94720 USA (e-mail: dleuen@eecs.berkeley.edu).

M.-C. M. Lee is with the Department of Electrical Engineering and the Institute of Photonics Technologies, National Tsing Hua University, Hsinchu 30055, Taiwan, R.O.C. (e-mail: mclee@ee.nthu.edu.tw).

Digital Object Identifier 10.1109/JSTQE.2007.893743

1077-260X/$25.00 © 2007 IEEE

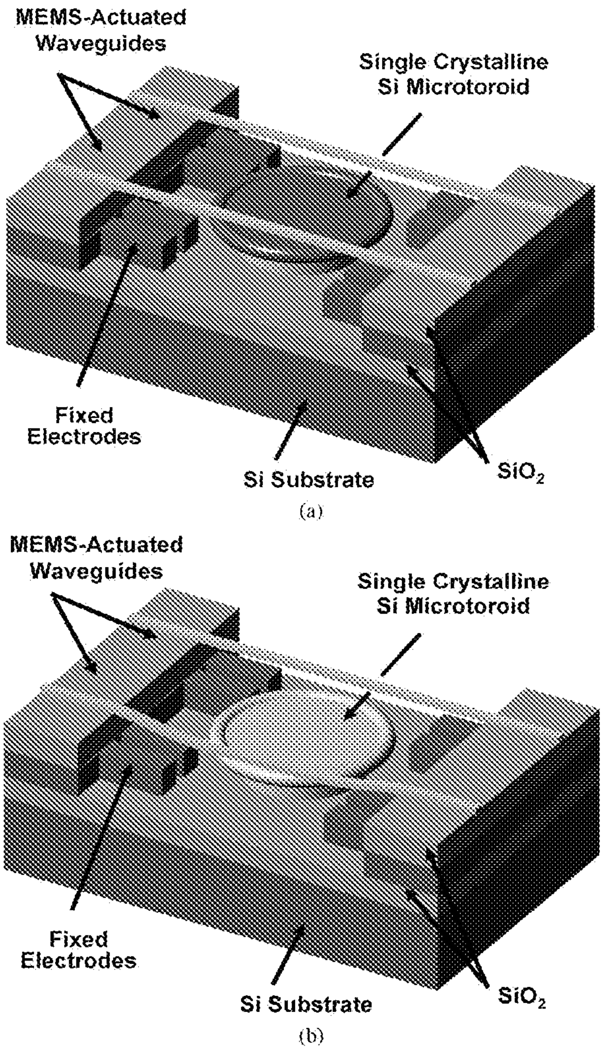

Fig. 1. (a) Schematic of the microtoroidal resonator with integrated MEMS tunable couplers. At zero bias, the initial spacing is large enough to ensure negligible coupling between the resonator and the waveguide coupler. (b) Schematic of the microtoroidal resonator with integrated MEMS tunable couplers under biased actuation. Lower waveguide is pulled downward to increase coupling, while the upper waveguide remains straight (uncoupled).

waveguides is 1 μm. It is chosen so that there is negligible coupling at zero bias, as shown in Fig. 1(a). With increasing voltage bias between the waveguide and the fixed electrodes, the suspended waveguide is pulled down toward the microtoroid, increasing the optical coupling exponentially, as illustrated in Fig. 1(b).

This design enables us to bias the microtoroidal resonator in all coupling regimes: under-coupling, critical coupling, and over-coupling, or even decoupled from the waveguide bus. Details of the MEMS actuator design have been reported in [22].

There is a design tradeoff in the doping concentration of the Si device layers. High doping is desired for the MEMS actuation, while low doping is necessary to minimize the optical absorption due to free carriers. Fortunately, electrostatic actuation does not require low resistivity. With a doping concentration of 10^{14} cm^{-3} (n-type dopants), a resistivity of 10 $\Omega\cdot$cm and an optical loss smaller than 0.01 cm^{-1} can be achieved. This absorption coefficient corresponds to a Q of 10^8 for microresonators if it is the dominant loss.

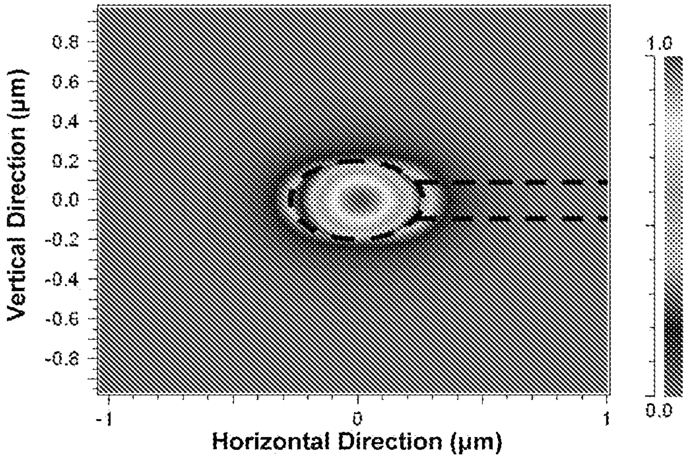

Fig. 2. Optical mode profile of the toroid for TE-like polarized light at 1.55 μm.

B. Waveguide Design for Phase Matching

Phase matching between the waveguide and the resonator is important to achieve an efficient coupling. Phase matching is satisfied when the two wave modes have the same propagation constant β.

We calculated the propagation constants of the microtoroid with the actual shape produced by hydrogen annealing using beam propagation method (BPM).[1] The optical field profile of the toroidal resonator at 1.55-μm wavelength is shown in Fig. 2. We used the following parameters in the calculation: refractive indexes of Si and air are 3.46 and 1.0, respectively; the bend radius of the toroid is 19.5 μm; and the radius of the toroid is 200 nm. It supports only one TE-like optical mode tightly confined to silicon.

Phase matching is achieved by controlling the dimensions of the waveguide. Fig. 3 shows the calculated propagation constants of the waveguide (lines) and the microtoroid (dots) versus wavelength for various waveguide dimensions. Here, we fix the waveguide width at 0.69 μm, the smallest linewidth that can regularly be produced by our lithography tool (10:1 reduction stepper). As shown in Fig. 3, the waveguide with 0.25-μm thickness is best matched to the microtoroid mode over a wide wavelength range around 1550 nm.

C. Fabrication Process

Our vertically coupled tunable microresonator was fabricated on a two-layer SOI using the wafer bonding process. The main challenge, here, was the nonplanar topography of the microtoroids that prevents the tight contact necessary for wafer bonding. We solved this problem by thinning the edges of the microdisks before hydrogen annealing so that the microtoroid surface was lower than the surrounding planar area. The detailed

---

[1] http://www.rsoftdesign.com/products/component_design/BeamPROP/

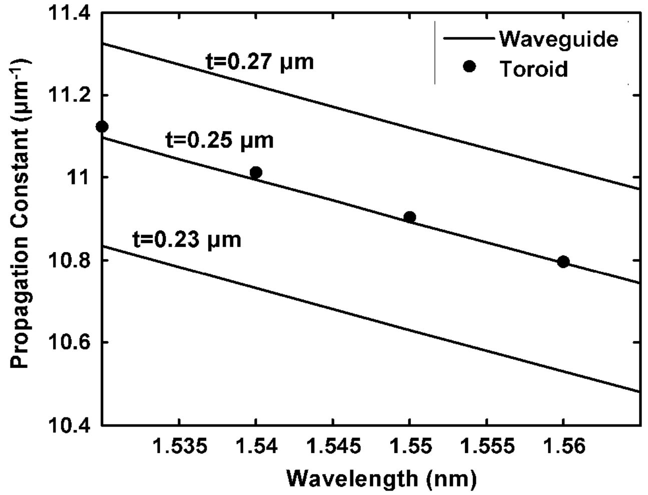

Fig. 3. Calculated propagation constants of the waveguide and the microtoroid versus wavelengths for various waveguide thicknesses, *t*. The width of the waveguide is fixed at 0.69 μm.

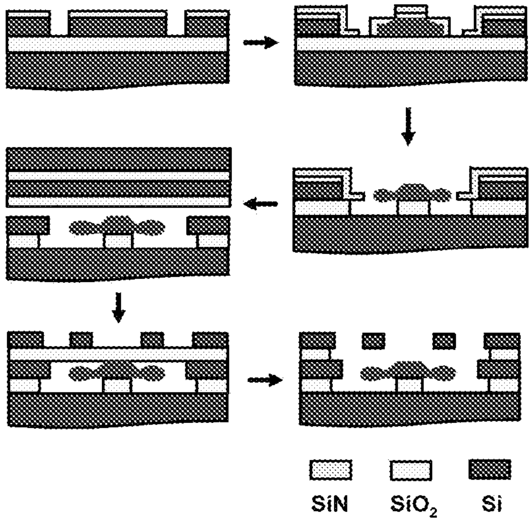

Fig. 4. Fabrication process for the tunable microtoroidal resonator.

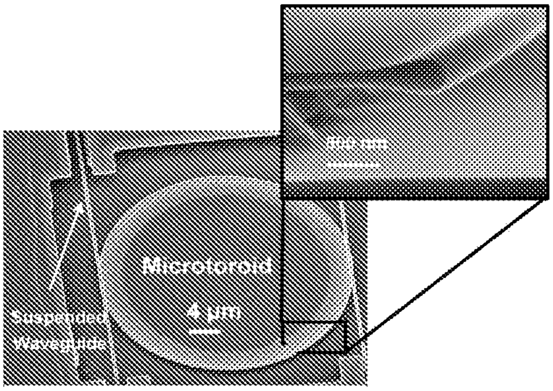

Fig. 5. SEM of the microtoroidal resonator and the suspended waveguides. Inset shows the cross-sectional view of the microtoroid.

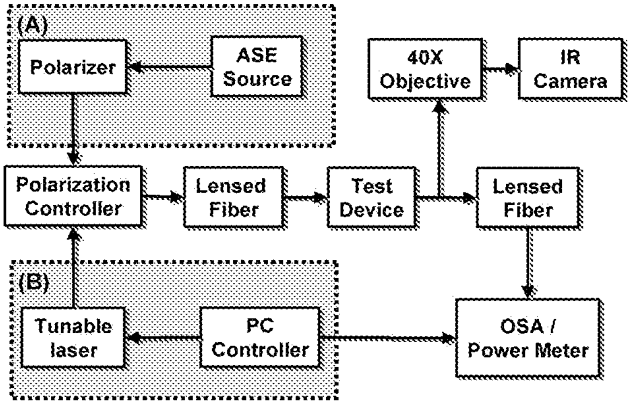

Fig. 6. Experimental setup for optical characterization. Amplified spontaneous emission (ASE) source is used (a) for quick measurement of the spectral response and (b) while the tunable laser provides high-resolution characterization.

fabrication process is shown in Fig. 4. First, microdisks were patterned and etched on an SOI wafer with a 350-nm-thick device layer. The edges of the disks were thinned down to 200 nm by thermal oxidation. This allowed room for the microtoroids to expand in the vertical direction during hydrogen annealing. The sample was then partially released in buffered HF and annealed in 10-Torr hydrogen ambient at 1050 °C for 5 min, creating a toroidal rim around the disks. The hydrogen annealing condition was optimized for the formation of the microtoroids, as reported in [24], [25]. A second SOI wafer with a 700-nm-thick device layer was thermally oxidized to create a SiO_2 spacer of 1-μm thickness. After oxidation, the thickness of the device layer was reduced to 250 nm. The toroid wafer was then fusion-bonded to the SOI wafer, whose substrate was subsequently removed to reveal the second SOI layer. The microtoroids were visible through the thin SOI layer, and the waveguide patterns were aligned to the edges of the underneath microtoroids. Finally, the waveguides around the toroids were released in buffered HF and supercritical dryer. In addition to creating a toroidal shape, the hydrogen annealing also reduced the surface roughness (to < 0.26 nm as reported in [26]), which was critical to attain high Q.

The scanning electron micrograph (SEM) of the fabricated device is shown in Fig. 5. The dimensions of the waveguides are measured to be 0.69-μm wide and 0.25-μm thick, very close to the designed parameters. The resonator exhibits a very smooth sidewall.

III. OPTICAL CHARACTERIZATION

The optical performance of the tunable microtoroidal resonator is tested using either a broadband amplified spontaneous emission (ASE) source (OpticWave Mini BLS-C-13) or a tunable laser (Agilent 81680A), as shown in Fig. 6. Light is coupled to the waveguides by polarization-maintaining lensed fibers. A calibrated optical power meter (HP 8153A) and an optical spectrum analyzer (OSA) (ANDO AQ6317B) are placed at the output to measure the transmitted power. The ASE provides a broadband source for quick measurement over a wide spectral range, while the tunable laser is used for high-resolution characterization. We have used TE-polarized input, which is attained by a linear polarizer and a polarization controller.

To actuate the waveguide, a voltage bias is applied to the fixed electrodes while the waveguide is grounded. At zero bias, almost

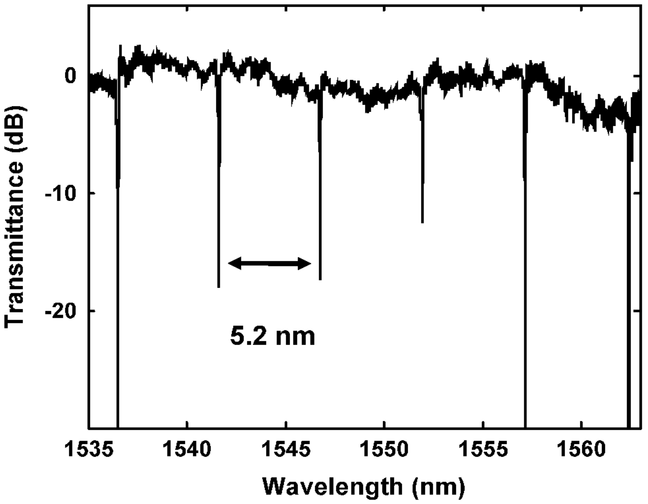

Fig. 7. Measured optical spectrum of a microtoroidal resonator at a bias voltage of 67 V. Measured free spectral range (FSR) of the TE mode is 5.2 nm.

100% of the light is transmitted to the output port. With increasing bias, sharp dips gradually appear in the transmission spectrum (Fig. 7). Each dip corresponds to a resonance wavelength. The free spectral range (FSR) of the TE mode is measured to be 5.2 nm. The small ripples are due to the reflections from the cleaved facets (Fabry–Perot effect). They can be eliminated by antireflection coating of the facets. Only a resonance peak is observed within each FSR, confirming the successful suppression of multiple radial modes observed in microdisk resonators.

The integrated tunable coupler enables the microresonator to operate in all coupling regimes. At low voltage, the microresonator is under-coupled. Fig. 8(a) shows the normalized transmission spectra of the resonator around one of the resonant wavelengths at 1548.2 nm at bias voltages of 51.0, 56.0, and 64.8 V. As the voltage increases, the optical coupling becomes stronger, leading to a larger dip at resonance. The three coupling regimes are clearly visible in Fig. 8(b), which plots the normalized transmittance at the resonant wavelength changes as a function of the applied voltage. In the under-coupling regime ($V_{\text{bias}} < 114$ V), the transmittance decreases continuously with the increasing voltage. The transmittance reaches a minimum at critical coupling ($V_{\text{bias}} = 114$ V). The extinction ratio is measured to be 22.4 dB at critical coupling. Further increase in voltage moves the resonator into the over-coupling regime. The increase in transmittance is accompanied by a broadening of the resonance linewidth since the coupling to waveguide is now stronger than the intrinsic loss of the resonator.

IV. THEORETICAL MODELING AND ANALYSIS

According to the time-domain coupling theory [1], the optical transfer function of the microresonator can be expressed as a function of resonant frequency (ω_0) and amplitude decay time constants τ_0 and τ_e, due to intrinsic loss and external coupling respectively

$$t_{\text{res}} = \frac{j(\omega - \omega_0) + \frac{1}{\tau_0} - \frac{1}{\tau_e}}{j(\omega - \omega_0) + \frac{1}{\tau_0} + \frac{1}{\tau_e}} \tag{1}$$

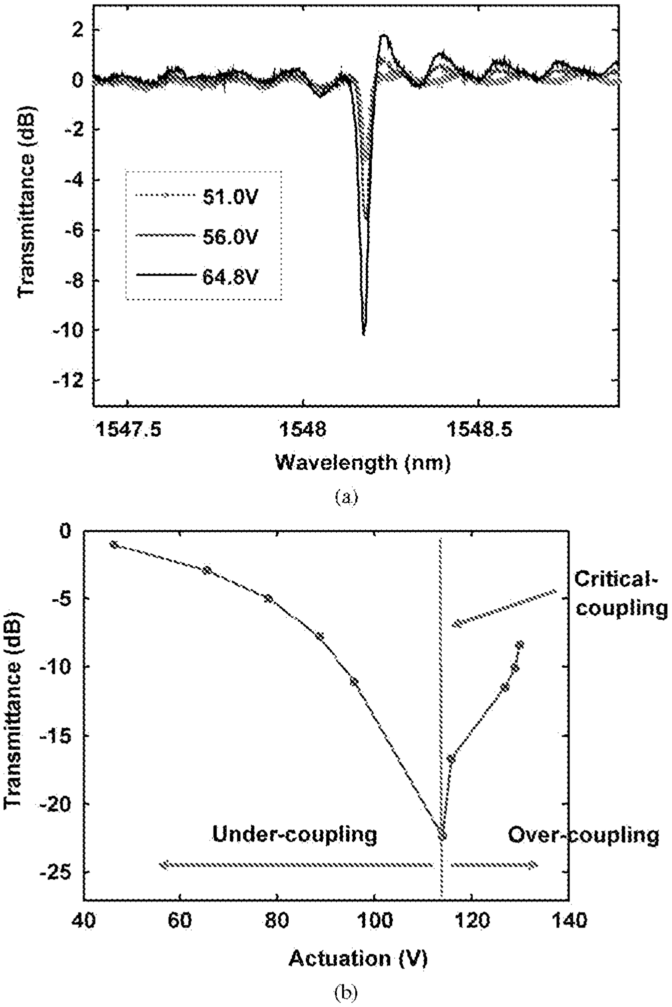

Fig. 8. (a) Measured normalized optical spectra of a microtoroidal resonator at bias voltages of 51.0, 56.0, and 64.8 V. (b) Normalized transmittance at resonance versus actuation voltage. Microresonator can be tuned continuously from under-coupling regime to over-coupling regime.

where t_{res} is the amplitude transfer function of the microresonator.

Alternatively, the transfer function can also be expressed in terms of the unloaded quality factor Q_0 and the external quality factor Q_e

$$t_{\text{res}} = \frac{2j\left(\frac{\lambda_0 - \lambda}{\lambda}\right) + \left(\frac{2}{Q_0} - \frac{1}{Q_L}\right)}{2j\left(\frac{\lambda_0 - \lambda}{\lambda}\right) + \left(\frac{1}{Q_L}\right)} \tag{2}$$

where $Q_0 = \omega_0 \tau_0 / 2$, $Q_e = \omega_0 \tau_e / 2$, and the loaded quality factor Q_L is defined as

$$\frac{1}{Q_L} = \frac{1}{Q_0} + \frac{1}{Q_e} \tag{3}$$

The measured spectra are usually complicated by the Fabry–Perot resonance between the two cleaved facets, as illustrated in Fig. 9. To model the measured spectrum more precisely, and extract the Q values of the resonator more accurately, particularly when the resonance peak is small, we develop a comprehensive

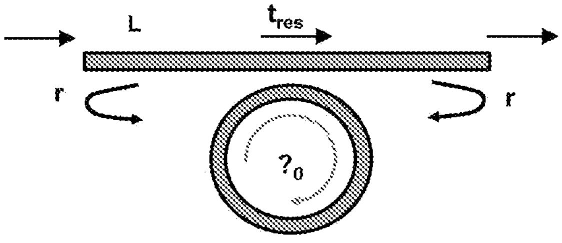

Fig. 9. Schematics illustrating the interaction between the microresonator and the Fabry–Perot resonance of the coupling waveguide.

model that includes both the effect of the microresonator and the Fabry–Perot ripples.

The total transmission t_{tot} is now a summation of multiple transmissions through the waveguide, as shown in

$$\begin{aligned} t_{\text{tot}} &= (1-r)^2 \exp(-\alpha L) \exp(jkLn_{\text{eff}}) t_{\text{res}} \\ &\quad + (1-r)^2 r^2 \exp(-3\alpha L) \exp(j(3kLn_{\text{eff}} + 2\phi_{\text{R}})) t_{\text{res}}^3 \\ &\quad + (1-r)^2 r^4 \exp(-5\alpha L) \exp(j(5kLn_{\text{eff}} + 4\phi_{\text{R}})) t_{\text{res}}^5 \\ &\quad + L \end{aligned} \tag{4}$$

where r is the amplitude reflection coefficient at the facet of the silicon waveguide, α is the optical loss per unit length in the waveguide, L is the length of the waveguide, k is the free-space propagation constant, n_{eff} is the effective refractive index of the Si waveguide, and ϕ_{R} is the optical phase change at the reflection per interface. Since there is a π phase shift at the reflection interface, the total transmission t_{tot} can be simplified to

$$\begin{aligned} t_{\text{tot}} &= (1-r)^2 \exp(-\alpha L) \exp(jkLn_{\text{eff}}) t_{\text{res}} \\ &\quad \{1 + r^2 \exp(-2\alpha L) \exp(j2kLn_{\text{eff}}) t_{\text{res}}^2 \\ &\quad + r^4 \exp(-4\alpha L) \exp(j4kLn_{\text{eff}}) t_{\text{res}}^4 + L\} \\ &= a_0(1 + q + q^2 + q^3 + L) \\ &= \frac{a_0}{1-q} \end{aligned} \tag{5}$$

where $a_0 = (1-r)^2 \exp(-\alpha L) \exp(jkLn_{\text{eff}}) t_{\text{res}}$, and $q = r^2 \exp(-2\alpha L) \exp(j2kLn_{\text{eff}}) t_{\text{res}}^2$.

In this derivation, we have assumed that the backscattering effect is small and can be neglected. The total intensity transmittance is then given by

$$T_{\text{res}} = |t_{\text{tot}}|^2 \tag{6}$$

To include the effect of waveguide dispersion, the phase factor kLn_{eff} is replaced by

$$\begin{aligned} \phi &= kL \left[n_{\text{eff}} + \frac{dn}{d\lambda}(\lambda - \lambda_0) \right] \\ &= kLn_{\text{eff}} \left[1 + \frac{dn}{d\lambda}\frac{1}{n_{\text{eff}}}(\lambda - \lambda_0) \right] \\ &= kLn_{\text{eff}} \left[1 + D_\lambda(\lambda - \lambda_0) \right] \end{aligned} \tag{7}$$

where $D_\lambda = \frac{dn}{d\lambda}\frac{1}{n_{\text{eff}}}$.

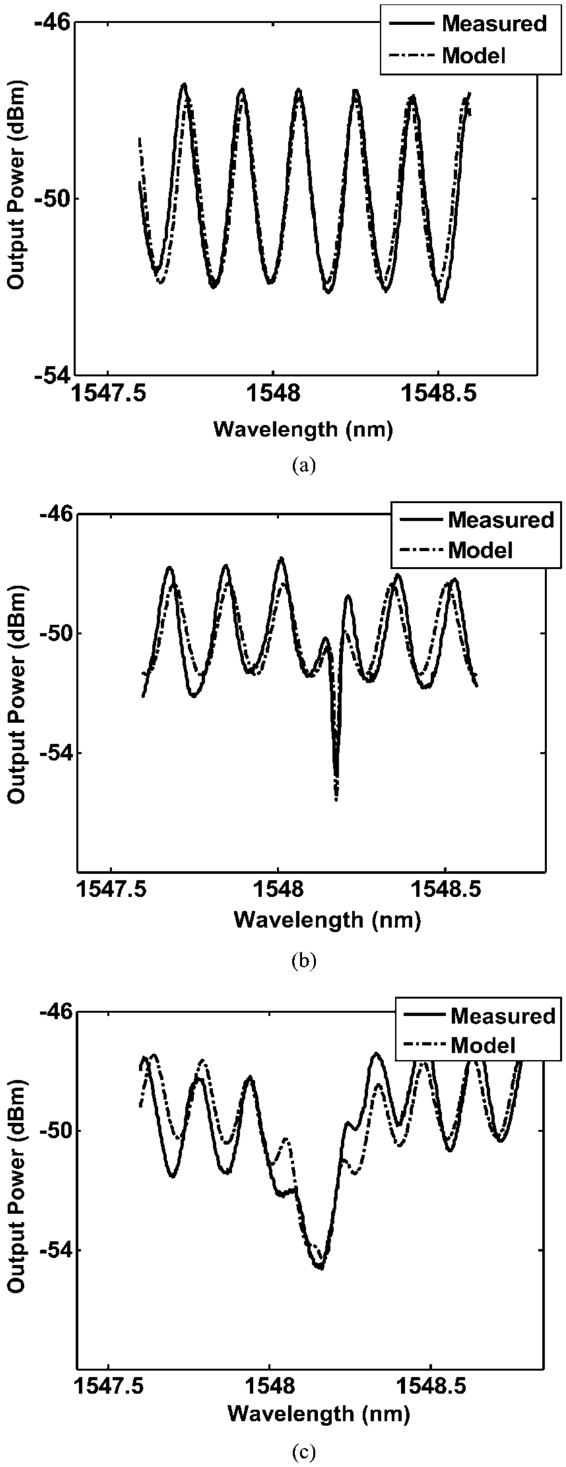

Fig. 10. (a) Measured and modeled spectra at 0 V (microresonator is decoupled). (b) Measured and modeled spectra at 64.8 V (microresonator is undercoupled). (c) Measured and modeled spectra at 130 V (microresonator is overcoupled).

The quality factors Q_0 and Q_L are extracted from the measured optical spectra by least-mean-square-error fitting to the model. Fig. 10 shows the measured and the fitted spectra around the resonance peak at 1548.2 nm when the resonator is:

a) decoupled; b) under-coupled; and c) over-coupled. The experimental data agree very well with the theoretical model. From the fitted spectral response, the unloaded quality factor Q_0 of the microtoroidal resonator is extracted to be 110 000. The loaded Q, i.e., Q_L, is continuously tunable from 110 000 to 5400, exhibiting a tuning ratio of more than 20:1.

The model described in this paper fit not only the resonance peak but also the ripples due to Fabry–Perot resonance. The quality factor extracted by this method is more accurate than by the lumped resonator model alone [27], especially when the resonance peak is small.

V. Discussion

Hydrogen annealing is a simple and powerful technique to fabricate suspended microring resonators with high-quality factor and single radial mode. Comparing the etched ring with tethered anchor [17], the seamless toroidal structure has lower scattering loss and higher Q. The hydrogen annealing process also greatly reduces the surface roughness, as confirmed by the high Q measured in our devices. These tunable microresonators described in this paper can be cascaded to form reconfigurable optical add–drop multiplexers, wavelength-selective switches, and crossconnects. It can also be used for bandwidth-tunable filters in dynamic optical networks. With the successful suppression of multiple radial modes, we expect the microtoroidal resonator to have even larger bandwidth tuning ratio than the microdisk-based filters in [28].

VI. Conclusion

We have successfully demonstrated a novel single crystalline silicon microtoroidal resonator with MEMS-actuated tunable optical coupler. It is fabricated by combining the hydrogen annealing and the wafer bonding processes. We have achieved an unloaded Q of 110 000 for a 39-μm-diameter resonator with a toroidal radius of 200 nm. The device is able to operate in all the three coupling regimes: under-, critical, and over-coupling. The resonator can also be decoupled from the waveguide, allowing them to be cascaded without loading the waveguides. We have developed a detailed model combining the time-domain coupling theory with the Fabry–Perot resonance of the waveguide. The experimental and the theoretical results agree very well. The loaded Q is continuously tunable from 110 000 to 5400. This device has potential applications in variable-bandwidth filters, reconfigurable add–drop multiplexers, wavelength-selective switches and crossconnects, and optical sensors.

Acknowledgment

The authors would like to thank the staff of the Microfabrication Laboratory, University of California, Berkeley. Part of the fabrication process was performed at Stanford Nanofabrication Facility, Stanford University. In particular, they would also like to acknowledge the assistance of M. Stevens and M. Mansourpour. They would also like to thank Dr. S. Mathai of the University of California, Berkeley, for helpful discussions and technical assistance.

References

[1] B. E. Little, S. T. Chu, H. A. Haus, J. Foresi, and J. P. Laine, "Microring resonator channel dropping filters," *J. Lightw. Technol.*, vol. 15, no. 6, pp. 998–1005, Jun. 1997.

[2] S. J. Choi, K. Djordjev, S. J. Choi, and P. D. Dapkus, "Microdisk lasers vertically coupled to output waveguides," *IEEE Photon. Technol. Lett.*, vol. 15, no. 10, pp. 1330–1332, Oct. 2003.

[3] Q. Xu, B. Schmidt, S. Pradhan, and M. Lipson, "Micrometre-scale silicon electro-optic modulator," *Nature*, vol. 435, no. 7040, pp. 325–327, May 2005.

[4] B. E. Little, S. T. Chu, W. Pan, and Y. Kokubun, "Microring resonator arrays for VLSI photonics," *IEEE Photon. Technol. Lett.*, vol. 12, no. 3, pp. 323–325, Mar. 2000.

[5] C. K. Madsen, G. Lenz, A. J. Bruce, M. A. Cappuzzo, L. T. Gomez, T. N. Nielsen, L. E. Adams, and I. Brenner, "An all-pass filter dispersion compensator using planar waveguide ring resonators," in *Proc. Opt. Fiber Commun. Conf. Int. Conf. Integr. Opt. Opt. Fiber Commun. (OFC/IOOC)*, Piscataway, NJ, Feb. 1999, vol. 4, pp. 99–101.

[6] G. Lenz, B. J. Eggleton, C. K. Madsen, and R. E. Slusher, "Optical delay lines based on optical filters," *IEEE J. Quantum Electron.*, vol. 37, no. 4, pp. 525–532, Apr. 2001.

[7] T. J. Kippenberg, S. M. Spillane, D. K. Armani, and K. J. Vahala, "Ultralow-threshold microcavity Raman laser on a microelectronic chip," *Opt. Lett.*, vol. 29, pp. 1224–1227, Jun. 2004.

[8] F. Vollmer, S. Arnold, D. Braun, I. Teraoka, and A. Libchaber., "Multiplexed DNA quantification by spectroscopic shift of two microsphere cavities," *Biophys. J.*, vol. 85, pp. 1974–1979, Sep. 2003.

[9] A. M. Armani and K. J. Vahala, "Heavy water detection using ultra-high-Q microcavities," *Opt. Lett.*, vol. 31, no. 12, pp. 1896–1898, Jun. 2006.

[10] D. K. Armani, T. J. Kippenberg, S. M. Spillane, and K. J. Vahala, "Ultra-high-Q toroid microcavity on a chip," *Nature*, vol. 421, pp. 925–929, Feb. 2003.

[11] M. Borselli, T. Johnson, and O. Painter, "Beyond the Rayleigh scattering limit in high-Q silicon microdisks: theory and experiment," *Opt. Express*, vol. 13, no. 5, pp. 1515–1530, Mar. 2005.

[12] A. Yariv, "Critical coupling and its control in optical waveguide-ring resonator systems," *IEEE Photon. Technol. Lett.*, vol. 14, no. 4, pp. 483–485, Apr. 2002.

[13] V. B. Braginsky, M. L. Gorodetsky, and V. S. Ilchenko, "Quality-factor and nonlinear properties of optical whispering-gallery modes," *Phys. Lett. A*, vol. 137, pp. 393–397, May 1989.

[14] J. C. Knight, G. Cheung, F. Jacques, and T. A. Birks, "Phase-matched excitation of whispering-gallery-mode resonances by a fiber taper," *Opt. Lett.*, vol. 22, pp. 1129–1131, Aug. 1997.

[15] M. Cai, O. Painter, and K. J. Vahala, "Observation of critical coupling in a fiber taper to a silica-microsphere whispering-gallery mode system," *Phys. Rev. Lett.*, vol. 85, pp. 74–77, Jul. 2000.

[16] M. Borselli, K. Srinivasan, P. E. Barclay, and O. Painter, "Rayleigh scattering, mode coupling, and optical loss in silicon microdisks," *Appl. Phys. Lett.*, vol. 85, pp. 3693–3695, 2004.

[17] L. Martinez and M. Lipson, "High confinement suspended micro-ring resonators in silicon-on-insulator," *Opt. Express*, vol. 14, no. 13, pp. 6259–6263, Jun. 2006.

[18] S. T. Chu, W. Pan, S. Sato, T. Kaneko, Y. Kokubun, and B. E. Little, "Wavelength trimming of a microring resonator filters by means of a UV sensitive polymer overlay," *IEEE Photon. Technol. Lett.*, vol. 11, no. 6, pp. 688–690, Jun. 1999.

[19] D. K. Sparacin, J. P. Lock, C. Hong, K. K. Gleason, L. C. Kimerling, and J. Michel, "Trimming of microring resonators using photo-oxidation of a plasma-polymerized organosilane cladding material," *Opt. Lett.*, vol. 30, no. 17, pp. 2251–2253, 2005.

[20] W. M. J. Green, R. K. Lee, G. DeRose, A. Scherer, and A. Yariv, "Hybrid InGaAsP-InP Mach-Zehnder racetrack resonator for thermooptic switching and coupling control," *Opt. Exp.*, vol. 13, pp. 1651–1659, Mar. 2005.

[21] M.-C. M. Lee and M. C. Wu, "MEMS-actuated microdisk resonators with variable power coupling ratios," *IEEE Photon. Technol. Lett.*, vol. 17, no. 5, pp. 1034–1036, May 2005.

[22] M.-C. M. Lee and M. C. Wu, "Tunable coupling regimes of silicon microdisk resonators using MEMS actuators," *Opt. Exp.*, vol. 14, no. 11, pp. 4703–4712, May 2006.

[23] U. Levy *et al.*, "On-chip microfluidic tuning of an optical microring resonator," *Appl. Phys. Lett.*, vol. 88, pp. 111107–111109, Mar. 2006.

[24] M.-C. M. Lee and M. C. Wu, "Thermal annealing in hydrogen for 3-D profile transformation on silicon-on-insulator and sidewall roughness reduction," *J. Microelectromech. Syst.*, vol. 15, no. 2, pp. 338–343, Apr. 2006.

[25] J. Yao, M.-C. M. Lee, and M. C. Wu, "Hydrogen annealing and bonding processes for integrated MEMS tunable microtoroidal resonators," to be published.

[26] M.-C. M. Lee, J. Yao, and M. C. Wu, "Silicon profile transformation and sidewall roughness reduction using hydrogen annealing," in *Proc. 18th IEEE Int. Conf. Microelectromech. Syst.*, Miami, FL, Jan. 30–Feb. 3, 2005, pp. 596–599.

[27] J. Yao, M.-C. M. Lee, D. Leuenberger, and M. C. Wu, "Silicon microtoroidal resonators with integrated MEMS tunable optical coupler," in *Proc. IEEE Opt. Microelectromech. Syst.*, Big Sky, MT, 2006, pp. 17–18.

[28] J. Yao, M.-C. M. Lee, D. Leuenberger, and M. C. Wu, "Wavelength- and bandwidth-tunable filters based on MEMS-actuated microdisk resonators," in *Proc. Opt. Fiber Commun. Conf. Nat. Fiber Opt. Eng. Long.*, Anaheim, CA, Mar. 5–10, 2006, p. 3.

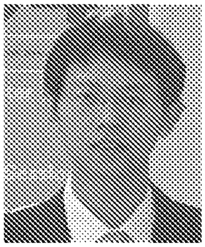

Jin Yao received the B.S. and M.S. degrees in electronic engineering from Tsinghua University, China, in 2000 and 2002, respectively. He is currently working toward the Ph.D. degree from the Department of Electrical Engineering and Computer Sciences, University of California, Berkeley.

His current research is focussed on silicon-based integrated microresonators, including design, simulation, fabrication, characterization, and their applications. His research interests include silicon-based photonic integrated circuits and micro-nano scale MEMS.

Mr. Yao won the California NanoSystems Institute (CNSI) Fellowship Award, in 2002–2003.

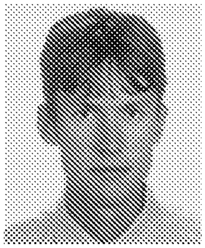

David Leuenberger received the graduate degree from the Institute of Applied Physics, University of Bern, Switzerland, in 2000. He received the Ph.D. degree from the Swiss Federal Institute of Technology, Lausanne, Switzerland, in 2004.

Currently, he is a Postdoctoral Researcher with the Integrated Photonics Laboratory, University of California, Berkeley. His current research interests include integrated microresonators for optical communication and sensing applications and optical antennas for surface enhanced Raman scattering. He is the author or coauthor of five journal papers and five conference papers.

Dr. Leuenberger is a member of the Optical Society of America (OSA).

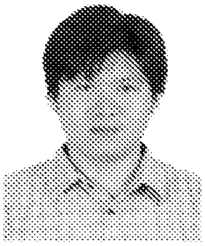

Ming-Chang M. Lee (S'04–M'05) was born in Taiwan, R.O.C. He received the B.S. degree in control engineering from the National Chiao Tung University, Hsinchu, Taiwan and the M.S. degree in electrical engineering from the National Taiwan University, Taipei, Taiwan, in 1994 and 1996, respectively. He received the Ph.D. degree in electrical engineering from the University of California, Los Angeles, in 2005.

Currently, he is with the faculty at the Institute of Photonics Technologies and the Department of Electrical Engineering, National Tsing Hua University, Taiwan. His research interests include optical MEMS, studies of nanophotonics, and the development of integrated photonic devices for optical communication and sensing.

Dr. Lee is a member of the Optical Society of America (OSA).

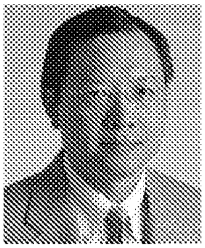

Ming C. Wu (S'82–M'83–SM'00–F'02) received the B.S. degree from National Taiwan University, Taipei, Taiwan, in 1983, and the M.S. and Ph.D. degrees from the University of California, Berkeley, in 1985 and 1988, respectively, all in electrical engineering.

Currently, he is a Professor of electrical engineering and computer sciences at the University of California, Berkeley, and a Co-Director of Berkeley Sensors and Actuators Center (BSAC). From 1988 to 1992, he was a Technical Staff at AT&T Bell Laboratories, Murray Hill, NJ. From 1993 to 2004, he was a Professor of electrical engineering at the University of California, Los Angeles (UCLA). He was also the Director of Nanoelectronics Research Facility and Vice Chair for Industrial Relations during his tenure at UCLA. In 1997, he cofounded OMM in San Diego, CA, to commercialize MEMS optical switches. He has published more than 400 papers, contributed five book chapters, and holds 11 U.S. patents. His research interests include optical MEMS, optoelectronics, and biophotonics. He has also participated in many technical conferences. He was the Guest Editor of two IEEE/OSA JOURNAL OF LIGHTWAVE TECHNOLOGY Special Issues on Optical MEMS.

Dr. Wu was a Fellow of David and Lucile Packard Foundation, from 1992 to 1997. He was the founding Co-Chair of the IEEE/LEOS Summer Topical Meeting on Optical MEMS in 1996.